# Optimal Velocity and Power Split Control of Hybrid Electric Vehicles

Stephan Uebel, Nikolce Murgovski, Conny Tempelhahn, Bernard Bäker

***Abstract*—An assessment study of a novel approach is presented that combines discrete state-space Dynamic Programming and Pontryagin's Maximum Principle for online optimal control of hybrid electric vehicles (HEV). In addition to electric energy storage and gear, kinetic energy and travel time are considered states in this paper. After presenting the corresponding model using a parallel HEV as an example, a benchmark method with Dynamic Programming is introduced which is used to show the solution quality of the novel approach. It is illustrated that the proposed method yields a close-to-optimal solution by solving the optimal control problem over one hundred thousand times faster than the benchmark method. Finally, a potential online usage is assessed by comparing solution quality and calculation time with regard to the quantization of the state space.**

***Index Terms*—Optimal control, Pontryagin's Maximum Principle, Dynamic programming, velocity control, hybrid vehicles, energy management**

## NOMENCLATURE

| | |
|---|---|
| $s, t$ | Space coordinate and time. |
| $k$ | Index of discretized space coordinate. |
| $N_\mathrm{k}$ | Final index $k$. |
| $\omega$ | Crankshaft speed. |
| $v$ | Vehicle longitudinal velocity. |
| $\gamma$ | Gear ratio. |
| $m$ | Vehicle mass. |
| $\mathrm{c_a}, c_\alpha$ | Air drag and slope coefficient. |
| $\eta_\mathrm{g}$ | Efficiency of the gearbox. |
| $P_\mathrm{S}, P_\mathrm{S,e}$ | Chemical and electrical power of the storage. |
| $U, R$ | Storage voltage and resistance. |
| $F_\mathrm{E,d}, F_\mathrm{T,d}$ | Dissipative forces for engine and gearbox. |
| $\sigma, g$ | States: engine state (on/off) and gear. |
| $E_\mathrm{S}, E_\mathrm{V}$ | States: storage energy and kinetic energy. |
| $f_\mathrm{S}, f_\mathrm{V}, f_\mathrm{t}$ | State dynamics for the indexed state. |
| $\mathbf{x}_\mathrm{d}, \mathbf{x}_\mathrm{c}, \mathbf{x}$ | Vectors for discrete, continuous and all states. |
| $F_\mathrm{E}, F_\mathrm{M}, F_\mathrm{B}$ | Control signals: Forces of engine, motor and brake. |
| $u_\sigma$, $u_\mathrm{g}$ | Control signals for $\sigma$ and $g$ |
| $\mathbf{u}_\mathrm{d}, \mathbf{u}_\mathrm{c}, \mathbf{u}$ | Vectors for discrete, continuous and all control signals. |
| $\hat{\{\cdot\}}$ | Value or index of maximum. |
| $\{\cdot\}'$ | First derivative with respect to $s$. |
| $\Delta\{\cdot\}$ | Step size. |
| $\{\cdot\}^+$ | Value at the next instant. |

## I. INTRODUCTION

Hybrid electric vehicles (HEVs) are widely regarded as one of the most promising solutions to the mitigation of environmental issues caused by the ever-increasing usage of fossil fuels in transportation [18]. In addition to the internal combustion engine (ICE), HEV powertrains include one or more electric machines (EMs) and an electric storage, typically a battery. This provides an additional source of power for propulsion which can be exploited to decrease the fossil fuel consumption by 1) recuperating braking energy that can be stored in the battery for later use, 2) shutting down the ICE during idling and low power demands and 3) operating the ICE at more efficient load conditions by storing the excess energy in the battery or assisting the ICE at high traction demands [13].

The fuel consumption and energy efficiency of an HEV depend crucially on the energy management strategy (EMS). For a certain gas pedal position and energy state of the vehicle, the EMS determines the split of demanded power between the power sources (ICE and EMs). Additionally, it may choose the ICE on/off state as well as the gear selection for powertrains with an automated gearbox. HEVs equipped with a telemetry system may further improve the energy efficiency by planning the anticipated power split over a receding horizon in front of the vehicle.

Large amount of scientific research has proposed EMS that controls three vehicle states, battery energy, gear and ICE on/off. Besides purely heuristic approaches, model-based control is the preferred implementation, where the EMS is coordinated by an optimal control algorithm. A comprehensive overview of different optimal, suboptimal and heuristic EMS for HEVs can be found in [19], [26].

Among the optimal control methods, Dynamic Programming (DP) is the one most commonly used ([24], [25], [31], [41], [42], [45], [49]), since DP can be easily applied to nonlinear, non-convex and mixed-integer control problems. However, a limitation of DP is the so-called *curse of dimensionality*, i.e. the computational effort increases exponentially with the number of state variables [1], which hinders the online usage (on-board the vehicle) of the algorithm.

With the aim of decreasing the computational effort, methods based on the Pontryagin's Maximum Principle (PMP) [36] have been proposed which adjoin the system dynamics to the objective. One of these well-known methods is the Equivalent Consumption Minimization Strategy (ECMS) [35] which simplifies the problem by neglecting the battery energy limits as well as by considering the gear and ICE on/off as control signals, rather than state variables [7], [15], [23], [27], [32]. Other methods retain the battery energy constraints, but require heuristics for the integer decisions. An example is the PMP method presented in [50] and the convex optimization methods proposed in [30], [38], [46].

To overcome the disadvantages of each single method, combinations of different optimization methods have also been suggested, which typically separate the integer from the real-valued decisions. For instance, the approach in [33] combines DP and PMP by disregarding battery energy limits

and regarding gear and ICE on/off as integer states. Similarly, [47] uses a combination of both methods to control the battery energy and the ICE on/off decision, by keeping battery energy limits in a series hybrid bus. Methods that combine convex optimization with either PMP or DP have been proposed in [9], [28], [34], [37]. These methods retain battery energy limits, while in the case of a combination with DP, gear and ICE on/off are also considered as integer states.

Besides the EMS, another factor that significantly affects the vehicle energy efficiency is the possibility to optimally control the kinetic and potential energy storage by varying the vehicle velocity in a hilly terrain, while satisfying the travel time given. For instance, a more efficient driving style can be achieved by decreasing velocity when climbing uphill and increasing velocity while rolling downhill, instead of wasting energy at the brake pads.

Improving energy efficiency by optimizing vehicle velocity has been applied to both conventional and hybrid vehicles. For instance, an early implementation for optimal velocity control of conventional passenger cars using DP for real-time application was presented by Porsche, called ACC InnoDrive [39]. Other approaches using DP concentrate on controlling velocity on short-range trips, e.g. the distance between two traffic lights [8], [48]. Using DP for both velocity control and gear shifting of conventional trucks has been proposed in [16], [17]. Furthermore, DP is used for optimal velocity control of truck platoons [6], but there, for the sake of computational efficiency, gear, ICE on/off and travel time are removed from the state vector, and the engine model is reduced to a simple constant efficiency.

Besides DP, other methods are examined for velocity control of conventional vehicles. For instance, convex quadratic programming has been proposed by [12]. A real-time capable, nonlinear predictive control approach for velocity control in urban areas is presented by [22]. Early research calculating the optimal velocity of a conventional vehicle with PMP was done by [43]. A combination of convex optimization and DP has been applied by [29] for optimal velocity control and gear selection for a platoon of conventional vehicles.

In comparison to velocity control of conventional vehicles, the velocity control of HEVs is more challenging due to the higher number of states. A comprehensive overview of publications dealing with this topic can be found in [44]. As hinted by [44], this is currently one of the topics most researched in the area of energy efficient vehicle control.

Despite the high number of states, real-time control using DP is possible when, for instance, the prediction horizon is short [53]. Nonetheless, it is not the preferred approach due to the high computational load of having the two real-valued states (velocity and battery energy) and possibly the two integer states (gear and engine on/off). Bosch developed a system called Eco-ACC which uses DP for an offline calculation of deceleration trajectories when drawing near a slower vehicle [10]. The results of DP are used to obtain lookup tables for a control unit implementation.

Approaches for velocity control of HEV using methods other than DP are also possible such as the ACC system for HEV trucks, presented by [51], in which the authors employ nonlinear optimization methods. In [52], a solution with PMP using a sum of piecewise affine continuous functions is presented. However, integer states are neglected and the model is restricted to strictly convex functions. Similarly, the procedure in [22] can be extended to control the power split in HEV as well. This method is used in [54] to optimize HEV trucks in a platoon.

Combinations of different methods are also investigated. An approach, published recently, decouples the integer from the real-valued decisions, so that DP selects gear and powertrain mode, while control of velocity and battery energy are chosen by convex optimization [20], [21]. However, model approximations may be required to derive a convex program [4].

In contrast to the previous approaches, this paper proposes a novel method for optimal control of velocity (kinetic energy), battery energy, engine state and gear of an HEV, without the need for a convex model. Sampling is performed in the space coordinate along the traveled distance, which introduces the travel time as a fifth state and allows hilly terrain of any shape to be included directly in the problem. To overcome the high computational burden associated with the travel time as a state, the approach in the present paper combines DP and PMP. DP controls the vehicle's kinetic energy and gear, given the costates for battery energy and travel time; wherein the costates are obtained by applying the PMP. Similar to most ECMS approaches, the single shooting method is used to solve a two-point boundary value problem (2PBVP). This ensures that final constraints on the battery energy and the travel time are met.

The proposed method provides the globally optimal solution when the battery energy limits are not activated. For other operating conditions, it has been observed that the proposed solution is close-to-optimal, with an error of less than 2.5 % in fuel consumption, compared to a benchmark solution obtained by DP. An online implementation of the novel algorithm is computationally feasible by using a rougher quantization of the state space, with the cost of increased fuel consumption compared to the offline solution.

This paper is organized as follows. The general optimal control problem is stated in Section II. Section III provides a benchmark solution obtained by solving a discrete state space DP. Section IV presents the proposed PMP-DP approach. Section V provides a case study in which the results of both the DP and the PMP-DP method are compared for different final state conditions. Section VI comes to a conclusion and gives an outline of ongoing research in the field.

## II. Problem Description

In this section, the problem is formulated for optimal energy management of an HEV. The method proposed is presented for an HEV powertrain in a parallel configuration [13, p. 61]. However, it is straightforward to apply the method to other powertrain concepts as well.

### A. Vehicle Model

The parallel HEV powertrain used in this study is illustrated in Fig. 1. The powertrain includes an ICE that converts

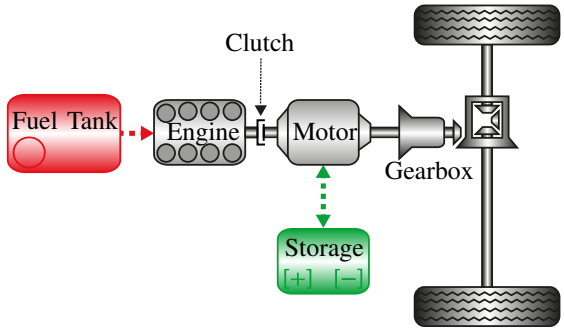


Fig. 1. Structure of a P2-HEV (according to [20]). It shows the energy flow from the fuel tank to the ICE which is connected with the EM. The storage delivers energy to the EM or receives energy from it. When the clutch is disengaged the engine is turned off. Otherwise the torques of ICE and EM add up. The resulting torque is transmitted by the gearbox to the wheels.

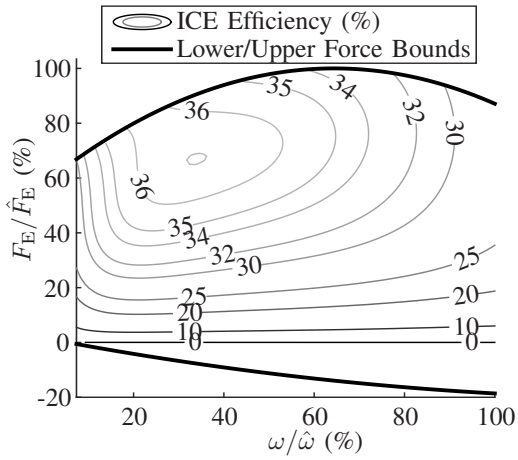


Fig. 2. Map of ICE efficiency and force bounds. Force and speed are given in terms of their maximum values $\hat{F}_E$ and $\hat{\omega}$.

chemical fuel energy to mechanical propulsion energy. The ICE is connected coaxially with an EM, which enables a hybrid mode of operation in which the ICE and the EM may split the necessary torque for propulsion. As energy storage, an electric battery is used, providing energy to the EM when the EM is in motoring mode, and receiving energy when the EM is in generating mode. This enables recuperation of energy when the vehicle is braking (decreasing kinetic energy) or going downhill (decreasing potential energy), and storing of excess energy in the battery when the ICE is delivering more torque than needed. Conversely, the ICE can be supported by the EM using the stored battery energy.

The ICE efficiency map, as a function of engine speed and torque, is provided in Fig. 2. It can be seen that engine efficiency drops significantly at low speed and torque. Therefore, the goal of the hybrid operation is to move the engine operating points at the higher efficiency area, or to turn the engine off and drive purely electrically. In order to remove engine friction losses in pure electric operation, the powertrain includes a clutch to disengage the ICE. The corresponding engine on/off state $\sigma$ is controlled by the binary signal $u_\sigma$. When $\sigma = 1$, distribution of both ICE torque ($T_E$) and EM torque ($T_M$) is possible. The direct connection ensures an identical rotational speed of both the ICE and the EM

$$\omega(v, g) = \frac{v}{\mathrm{r}}\gamma(g) \tag{1}$$

which depends on the longitudinal vehicle velocity $v$, the dynamic rolling radius of the wheels $\mathrm{r}$ and the gear ratio $\gamma(g)$. The latter is determined by the gear $g$ that is an integer system state controlled by the signal $u_g$. The two integer states form the discrete vector

$$\mathbf{x}_d = (\sigma, g) \tag{2}$$

while the corresponding vector of discrete control signals is denoted as

$$\mathbf{u}_d = (u_\sigma, u_g). \tag{3}$$

The ICE force $F_E = T_E/\mathrm{r}$, the EM force $F_M = T_M/\mathrm{r}$ and the mechanical brake force $F_B$ are control signals as well. They are gathered in the vector of continuous inputs

$$\mathbf{u}_c = (F_E, F_M, F_B), \tag{4}$$

which finally gives the entire input vector

$$\mathbf{u} = (\mathbf{u}_c, \mathbf{u}_d). \tag{5}$$

The forces $F_E$ and $F_M$ add up to a crankshaft force which the gearbox translates to a wheel force. The gearbox has an efficiency $\eta_g$ that determines its dissipative force

$$F_{T,d}(\mathbf{u}) = \begin{cases} (F_M + F_E\sigma)(\eta_g - 1)/\eta_g, & \text{for } F_M + F_E \leq 0 \\ (F_M + F_E\sigma)(1 - \eta_g), & \text{for } F_M + F_E > 0 \end{cases} \tag{6}$$

which counteracts the wheel force. The brake and the driving resistance due to inertia, air drag and road slope cause further counteracting forces. Accordingly, the balance of forces at the wheel is

$$\mathrm{m}v\frac{dv}{ds} + \mathrm{c_a}v^2 + c_\alpha + F_B = (F_M + F_E\sigma - F_{T,d}(\mathbf{u}))\gamma(g), \quad \forall s \in [\mathrm{s_0}, \mathrm{s_f}], \tag{7}$$

where $\mathrm{m}$ is the vehicle mass, $\mathrm{c_a}$ is a constant for the air drag and $c_\alpha$ a slope-dependent factor. The balance is formulated in a space coordinate $s$, which denotes the travelled distance starting from an initial position $\mathrm{s_0}$ to a final position $\mathrm{s_f}$. The term $vdv/ds$ in (7) derives directly from the time to space transformation

$$\frac{dv}{dt} = v\frac{dv}{ds}. \tag{8}$$

Note that, for brevity, the dependency on $s$ is not displayed. All states and control signals and some coefficients in this paper depend on $s$. Constants that do not depend on $s$ are displayed in upright letters. For instance in (7), $\mathrm{c_a}$ does not depend on $s$ while $c_\alpha$ does.

It can be noticed that the state dynamics in (7) are nonlinear. A straightforward way to remove nonlinearity, without introducing approximations, is to perform a variable change, where kinetic energy

$$E_V = \frac{1}{2}mv^2 \tag{9}$$

is used as system state instead of longitudinal velocity. In space domain, the derivative of vehicle energy transforms into

$$\frac{\partial E_{\mathrm{V}}}{\partial s} = E'_{\mathrm{V}} = \frac{1}{2}\mathrm{m}\frac{dv^2}{ds} = \mathrm{m}v\frac{dv}{ds} = \mathrm{m}vv', \tag{10}$$

where the prime symbol ( $'$ ) is used as a shorthand notation for the first derivative with respect to $s$. As a consequence, 10), (7) can be written as

$$\begin{aligned} &E'_{\mathrm{V}} = f_{\mathrm{V}}(\mathbf{u}, E_{\mathrm{V}}, g) = \\ &(F_{\mathrm{M}} + F_{\mathrm{E}}\sigma - F_{\mathrm{T,d}}(\mathbf{u}))\gamma(g) - F_{\mathrm{B}} - 2\mathrm{c_a}E_{\mathrm{V}}/\mathrm{m} - c_\alpha \\ &\in \mathrm{m}[\mathrm{a_{min}}, \mathrm{a_{max}}], \end{aligned} \tag{11}$$

which gives the state differential equation of the kinetic energy $f_{\mathrm{V}}$ that is limited by the minimum acceleration $\mathrm{a_{min}}$ and the maximum acceleration $\mathrm{a_{max}}$.

Since the problem is formulated in space coordinates, the travel time $t$ is introduced as a system state. Its state dynamics are expressed by

$$t' = 1/v = 1/\sqrt{2E_{\mathrm{V}}/\mathrm{m}} = f_{\mathrm{t}}(E_{\mathrm{V}}). \tag{12}$$

The battery energy $E_{\mathrm{S}}$ is a system state which is gathered with the other continuous states in the vector

$$\mathbf{x}_{\mathrm{c}} = (E_{\mathrm{S}}, E_{\mathrm{V}}, t) \tag{13}$$

which is included in the complete state vector

$$\mathbf{x} = (\mathbf{x}_{\mathrm{c}}, \mathbf{x}_{\mathrm{d}}) \tag{14}$$

together with the integer states. The battery energy dynamics are then described by

$$E'_{\mathrm{S}} = -P_{\mathrm{S}}(F_{\mathrm{M}}, \mathbf{x})/\sqrt{2E_{\mathrm{V}}/\mathrm{m}} = f_{\mathrm{S}}(F_{\mathrm{M}}, \mathbf{x}), \tag{15}$$

where the chemical (i.e. internal) battery power $P_{\mathrm{S}}$ is considered to be negative when charging.

The battery is modeled as a series connection of an ideal voltage source and an ohmic resistance (cf. [13, p. 97]). Accordingly, the chemical power

$$P_{\mathrm{S}}(F_{\mathrm{M}}, \mathbf{x}) = P_{\mathrm{S,d}}(F_{\mathrm{M}}, \mathbf{x}) + P_{\mathrm{S,e}}(F_{\mathrm{M}}, \mathbf{x}) \in [\mathrm{P_{Smin}}, \mathrm{P_{Smax}}], \tag{16}$$

which is limited by the constant bounds $\mathrm{P_{Smin}}$ and $\mathrm{P_{Smax}}$, is the sum of the dissipative power $P_{\mathrm{S,d}}$ and the battery terminal (electrical) power

$$P_{\mathrm{S,e}}(F_{\mathrm{M}}, \mathbf{x}) = P_{\mathrm{M}}(F_{\mathrm{M}}, \mathbf{x}) + P_{\mathrm{M,d}}(F_{\mathrm{M}}, \mathbf{x}) + P_{\mathrm{A}}. \tag{17}$$

In (17), the EM mechanical power is

$$P_{\mathrm{M}}(F_{\mathrm{M}}, \mathbf{x}) = T_{\mathrm{M}}(F_{\mathrm{M}})\omega(\mathbf{x}) = F_{\mathrm{M}}\sqrt{2E_{\mathrm{V}}/\mathrm{m}}\gamma(g), \tag{18}$$

where $P_{\mathrm{A}}$ is the auxiliary power and $P_{\mathrm{M,d}}(F_{\mathrm{M}}, \mathbf{x})$ is the EM dissipative power which is given as a static lookup table. Providing a more informative depiction, the lookup table in Fig. 3 shows the EM efficiency.

The battery losses

$$\begin{aligned} &P_{\mathrm{S,d}}(F_{\mathrm{M}}, \mathbf{x}) = \\ &\frac{\left(U(E_{\mathrm{S}}) - \sqrt{U^2(E_{\mathrm{S}}) - 4R(F_{\mathrm{M}}, \mathbf{x})P_{\mathrm{S,e}}(F_{\mathrm{M}}, \mathbf{x})}\right)^2}{4R(F_{\mathrm{M}}, \mathbf{x})} \end{aligned} \tag{19}$$

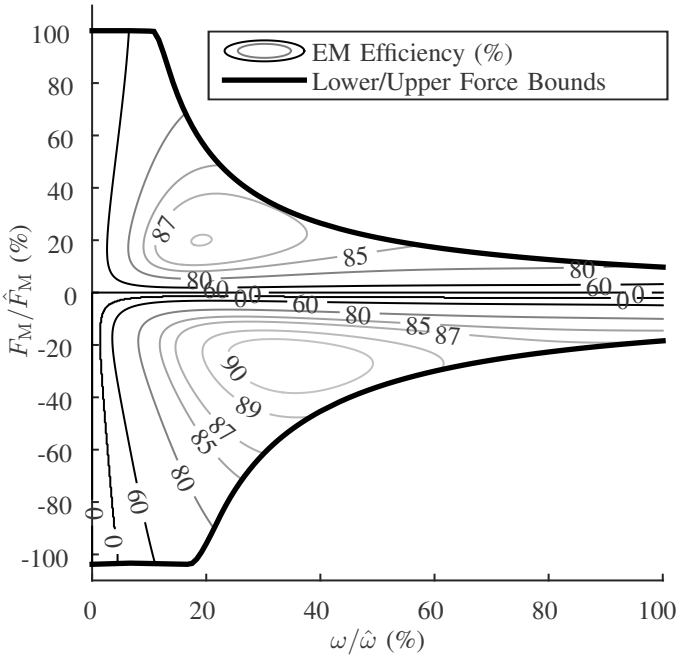


Fig. 3. Map of EM efficiency and force bounds. The force is given in terms of its maximum value $\hat{F}_{\mathrm{M}}$.

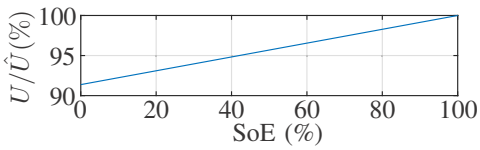


Fig. 4. Dependency of open-circuit voltage and the battery state of energy. The voltage is given in terms of its maximum value $\hat{U}$.

depend on the terminal power, the battery resistance $R(F_{\mathrm{M}}, \mathbf{x})$ and the open-circuit voltage $U(E_{\mathrm{S}})$, which is illustrated in Fig. 4. The abscissa shows the battery's state of energy (SoE), i.e. the battery energy normalized with respect to its maximum value. The resistance

$$R(F_{\mathrm{M}}, \mathbf{x}) = \begin{cases} \mathrm{R}_+, & \text{for } P_{\mathrm{S}}(F_{\mathrm{M}}, \mathbf{x}) \leq 0 \\ \mathrm{R}_-, & \text{for } P_{\mathrm{S}}(F_{\mathrm{M}}, \mathbf{x}) > 0 \end{cases} \tag{20}$$

may change value, depending on whether the battery is being charged or discharged.

### B. Problem Formulation

This section formulates the optimal control problem using the previously introduced model.

The main objective is to minimize fuel consumption for a given slope profile, subject to state and control constraints. The amount of fuel, expressed as consumed fuel energy, is the integrated sum of $F_{\mathrm{E}}$ and the dissipative ICE force $F_{\mathrm{E,d}}(F_{\mathrm{E}}, \mathbf{x})$ over $s$, which is provided by the lookup table illustrated in Fig. 2. In addition to the fuel energy, the objective is augmented with additional two terms

$$\mathcal{L}(\mathbf{u}, \mathbf{x}) = (F_{\mathrm{E}} + F_{\mathrm{E,d}}(F_{\mathrm{E}}, \mathbf{x}))\,\sigma\gamma(g) + |u_\sigma|\beta_\sigma + |u_{\mathrm{g}}|\beta_{\mathrm{g}} \tag{21}$$

where $\beta_\sigma$ and $\beta_{\mathrm{g}}$ are weights introduced to penalize driver discomfort and loss in energy due to frequently changing

engine state and gear, respectively. Hence, the optimal control problem is:

$$\text{minimize} \int_{\mathrm{s_0}}^{\mathrm{s_f}} \mathcal{L}(\mathbf{u}, \mathbf{x}) ds \tag{22a}$$

s.t.

$$\mathbf{x}_{\mathrm{c}}' = \mathbf{f}_{\mathrm{c}}(\mathbf{u}, \mathbf{x}) \tag{22b}$$
$$\mathbf{x}_{\mathrm{d}}^{+} = \mathbf{x}_{\mathrm{d}} + \mathbf{u}_{\mathrm{d}} \tag{22c}$$
$$\mathbf{x}(\mathrm{s_0}) = \mathbf{x}_0, \quad \mathbf{x}(\mathrm{s_f}) = \mathbf{x}_{\mathrm{f}} \tag{22d}$$
$$\mathbf{x} \in [\mathbf{x}_{\min}, \mathbf{x}_{\max}] \tag{22e}$$
$$\mathbf{u}_{\mathrm{c}} \in [\mathbf{u}_{\mathrm{c,min}}(\mathbf{x}), \mathbf{u}_{\mathrm{c,max}}(\mathbf{x})] \tag{22f}$$
$$u_\sigma, u_{\mathrm{g}} \in \{-1, 0, 1\}, \tag{22g}$$

where $\mathbf{x}_{\mathrm{d}}^{+}$ denotes the discrete states at the next space instant.

In problem (22), the function

$$\mathbf{f}_{\mathrm{c}}(\mathbf{u}, \mathbf{x}) = (f_{\mathrm{S}}, f_{\mathrm{V}}, f_{\mathrm{t}}) \tag{23}$$

combines the state dynamics of the continuous states. The initial and final state conditions are given by the vectors $\mathbf{x}_0$ and $\mathbf{x}_{\mathrm{f}}$, respectively. The state space is bounded by lower ($\mathbf{x}_{\min}$) and upper ($\mathbf{x}_{\max}$) limits. More specifically, the limits on $E_{\mathrm{S}}$ and $\mathbf{x}_{\mathrm{d}}$ are constant, while the limits on $E_{\mathrm{V}}$ and $t$ depend on $s$. Note that the limits of travel time and the bounds on kinetic energy depend on each other. For instance, the upper limit of $t$ can be derived from the lowest possible velocity, i.e. the lower bound on $E_{\mathrm{V}}$ and vice versa.

Similar to the states, the continuous inputs have lower and upper bounds expressed by $\mathbf{u}_{\mathrm{c,min}}(\mathbf{x})$ and $\mathbf{u}_{\mathrm{c,max}}(\mathbf{x})$, respectively. The bounds on the ICE force and the EM force shown in Fig. 2 and Fig. 3, respectively, depend on $\omega(v, g)$, and consequently, on the states $E_{\mathrm{V}}$ and $g$. The mechanical braking force $F_{\mathrm{B}} \in [0, \inf]$ is nonnegative.

**Remark 1.** *Since problem (22) is written in continuous space, a mathematically correct description is to replace the discrete control signals in the objective with a Dirac delta function that is non-zero only at instances where the integer decisions are nonzero. This slight abuse of notation has, however, a minor consequence, since in the reminder of the paper the problem is rewritten and solved in discrete space.*

**Remark 2.** *Alternative formulations of problem (22) exist where the terms multiplied by $\beta_\sigma$ and $\beta_{\mathrm{g}}$ are not present in the objective. Consequently, former decisions of $u_\sigma$ would not affect the fuel consumption and the engine state $\sigma$ could be removed from the problem, while $u_\sigma$ would simply take values in the set $\{0, 1\}$. Further simplifications, by e.g. removing the gear state, are not possible, unless the allowed gear shift set $\{-1, 0, 1\}$ is replaced with the set of all possible gears.*

## III. Benchmark Solution

This section reformulates problem (22) in discrete space and provides the optimal benchmark solution by implementing a discrete state-space DP.

DP uses Bellman's Principle of Optimality [1], [2], i.e. it computes the optimal solution by splitting the problem into subproblems. The principle states that when a trajectory $\Pi$ from an initial state to a final state is optimal, a trajectory from any intermediate state on $\Pi$ to the final state is also optimal as well as a trajectory from the initial state to any intermediate state on $\Pi$. This means that DP can be computed forward or backward in time (or more precisely in space, for problem formulation (22)).

In order to use DP, the hybrid (mixed-integer) control problem (22) is transformed into a purely integer problem by discretization of the space coordinate and quantization of the continuous states $\mathbf{x}_{\mathrm{c}}$ and control signals $\mathbf{u}_{\mathrm{c}}$. For brevity, the same symbols used in (22) represent discrete signals hereafter. Thus, the discrete problem formulation is

$$\text{minimize} \sum_{k=1}^{N_{\mathrm{k}}} \mathcal{L}(\mathbf{x}, \mathbf{u}) \Delta s \tag{24a}$$

s.t.

$$\mathbf{x}_{\mathrm{c}}(k+1) = \mathbf{x}_{\mathrm{c}}(k) + \mathbf{f}_{\mathrm{c}}(\mathbf{u}, \mathbf{x}) \Delta s \tag{24b}$$
$$\mathbf{x}_{\mathrm{d}}(k+1) = \mathbf{x}_{\mathrm{d}}(k) + \mathbf{u}_{\mathrm{d}} \tag{24c}$$
$$\mathbf{x}(0) = \mathbf{x}_0, \quad \mathbf{x}(N_{\mathrm{k}}) = \mathbf{x}_{\mathrm{f}} \tag{24d}$$
$$\mathbf{x} \in [\mathbf{x}_{\min}, \mathbf{x}_{\max}] \tag{24e}$$
$$\mathbf{u}_{\mathrm{c}} \in [\mathbf{u}_{\mathrm{c,min}}(\mathbf{x}), \mathbf{u}_{\mathrm{c,max}}(\mathbf{x})] \tag{24f}$$
$$u_\sigma, u_{\mathrm{g}} \in \{-1, 0, 1\}, \tag{24g}$$

in which $k$ denotes a discrete instant of $s$, $\Delta s$ is sampling interval and $N_{\mathrm{k}}$ is the total number of sampling instances. The reformulated problem (24) is solved with a discrete state-space DP. However, the vast state space leads to a high computational effort which prevents an online usage. Due to this, DP is used solely to benchmark the novel approach introduced hereafter.

## IV. PMP-DP Approach

A computationally efficient algorithm is proposed in this section by combining PMP and DP. First, PMP is applied on problem (22) in order to derive important properties of the optimal costate values. These propoerties are then used to propose the novel PMP-DP algorithm.

### A. PMP formulation of the problem

Following Pontryagin's maximum principle [11], [14], problem (22) can be solved by formulating the Hamiltonian

$$\mathcal{H}(\mathbf{x}, \boldsymbol{\psi}, \mathbf{u}) = \mathcal{L}(\mathbf{x}, \mathbf{u}) + \boldsymbol{\psi}^T \mathbf{f}_{\mathrm{c}}(\mathbf{u}, \mathbf{x}), \tag{25}$$

where the vector of Lagrange multipliers

$$\boldsymbol{\psi} = (\psi_{\mathrm{S}}, \psi_{\mathrm{V}}, \psi_{\mathrm{t}}) \tag{26}$$

includes the costates $\psi_{\mathrm{S}}$, $\psi_{\mathrm{V}}$ and $\psi_{\mathrm{t}}$, which relate to the continuous states $E_{\mathrm{S}}$, $E_{\mathrm{V}}$ and $t$, respectively. Hence, the problem is reformulated as

$$\text{minimize} \quad \mathcal{H}(\mathbf{x}, \boldsymbol{\psi}, \mathbf{u}) \tag{27a}$$

s.t.

$$\psi' = -\frac{\partial \mathcal{H}(\mathbf{x}, \boldsymbol{\psi}, \mathbf{u})}{\partial \mathbf{x}_\mathrm{c}} \tag{27b}$$

$$\mathbf{x}_\mathrm{d}(k+1) = \mathbf{x}_\mathrm{d}(k) + \mathbf{u}_\mathrm{d} \tag{27c}$$

$$\mathbf{x}(0) = \mathbf{x}_0, \quad \mathbf{x}(N_\mathrm{k}) = \mathbf{x}_\mathrm{f} \tag{27d}$$

$$\mathbf{x} \in [\mathbf{x}_\mathrm{min}, \mathbf{x}_\mathrm{max}] \tag{27e}$$

$$\mathbf{u}_\mathrm{c} \in [\mathbf{u}_\mathrm{c,min}(\mathbf{x}), \mathbf{u}_\mathrm{c,max}(\mathbf{x})] \tag{27f}$$

$$u_\sigma, u_\mathrm{g} \in \{-1, 0, 1\}, \tag{27g}$$

where (27b) is a necessary condition that has to be fulfilled if the continuous state constraints in (27e) are not activated at the optimum [11], [14]. The objective function changes from the Lagrange resolvent (22a) to a local minimization of the Hamiltonian (27a).

Under the assumption that the battery open circuit voltage variation (see Fig. 4) can be neglected [13, p. 214], it can be assumed that $\mathcal{H}(\mathbf{x}, \boldsymbol{\psi}, \mathbf{u})$ is not a function of $E_\mathrm{S}$, the battery costate would satisfy

$$\psi_\mathrm{S}' = -\frac{\partial \mathcal{H}(\mathbf{x}, \boldsymbol{\psi}, \mathbf{u})}{\partial E_\mathrm{S}} = 0 \tag{28}$$

at all instance where battery energy limits are not activated. Thus, if battery energy limits are never activated, $\psi_\mathrm{S}$ can be seen as constant, i.e. one scalar value that satisfies the final constraint on the battery energy. This is a widely used strategy, known in literature as the Equivalent Consumption Minimization Strategy (ECMS), where the scalar costate is obtained by solving a 2PBVP [23], [47], [50]. A disadvantage of ECMS is that it cannot prevent a violation of the battery energy limits in (27e), since the optimal costate might not be constant (even for a battery with constant open circuit voltage), but might change value each time the battery energy limits get activated. Several methods have been proposed in literature to resolve this issue, but besides the purely heuristic approaches, the method proposed by [50] can be seen as the most promising. Here, we adopt the approach by [50], where the problem is solved by recursively splitting the horizon into segments at instances where the battery energy limits would be most violated, if scalar battery costate would be used for the entire segment. The resulting solution is a piecewise constant battery costate, which is the globally optimal solution for certain types of convex energy management problems [50]. For generally non-convex problems, such as problem (24), it has been observed that the piecewise constant solution is close to the optimum [23].

The costate for the travel time is a constant scalar value for the entire driving cycle, because its differential equation

$$\psi_\mathrm{t}' = -\frac{\partial \mathcal{H}(\mathbf{x}, \boldsymbol{\psi}, \mathbf{u})}{\partial t} = 0 \tag{29}$$

is not dependent on the travel time. Moreover, following (12), the travel time is monotonically increasing and its state bounds are activated only at the beginning and the end of the horizon, so a horizon split is not necessary.

In contrast to $\psi_\mathrm{t}$ and $\psi_\mathrm{S}$, the costate for the kinetic energy $\psi_\mathrm{V}$ is not constant and there are no known approximations that can be used to obtain a close-to-optimal costate trajectory. A single shooting is in this case numerically unstable, due to a strong dependence on the initial value of the costate [3, p. 221]. Therefore, the following subsection introduces an approach to overcome this obstacle by combining DP with the costate properties (28) and (29) derived from PMP.

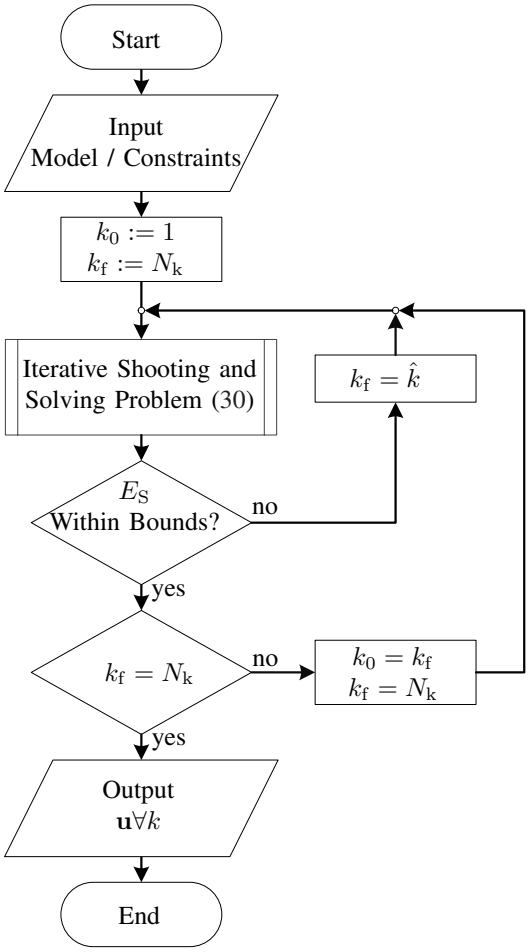


Fig. 5. Algorithm of PMP-DP approach. After initialization, problem (30) is solved iteratively for the full horizon in a subprogram which finds the values for the costates and outputs the state and control trajectories. Afterwards, it is checked if the bounds on the battery energy are activated, since the subprogram neglects the corresponding constraints. If the bounds on $E_\mathrm{S}$ are violated, the horizon is split at $\hat{k}$ which is the point where the bounds are exceeded the most. Subsequently, problem (30) is solved for the new segment. Note that the final state conditions are adapted, which is not displayed here. The segmentation is repeated until the battery energy does not violate the bounds. Following, the final position of the segment becomes the starting position of the next segment. After all segments are solved, the algorithm outputs the control trajectory.

### B. PMP-DP algorithm

The idea behind the novel approach is to use the Hamiltonian as the objective function for a discrete state space DP, where the states for battery energy and travel time are effectively removed from the problem, given the values for their corresponding costates ($\psi_\mathrm{S}$ and $\psi_\mathrm{t}$). The costates, in turn, are obtained by solving 2PBVP with horizon splitting as proposed by [50]. The resulting algorithm is illustrated in Fig. 5, where, the problem

$$\text{minimize} \sum_{k=k_0}^{k_\mathrm{f}} \mathcal{L}(\mathbf{x},\mathbf{u}) + \psi_\mathrm{S}\, f_\mathrm{S}(\mathbf{u},\mathbf{x}) + \psi_\mathrm{t}\, f_\mathrm{t}(\mathbf{u},\mathbf{x}) \tag{30a}$$

s.t.

$$E_\mathrm{V}(k+1) = E_\mathrm{V}(k) + f_\mathrm{V}\Delta s \tag{30b}$$
$$\mathbf{x}_\mathrm{d}(k+1) = \mathbf{x}_\mathrm{d}(k) + \mathbf{u}_\mathrm{d} \tag{30c}$$
$$\mathbf{x}(k_0) = \mathbf{x}_0, \quad \mathbf{x}(k_\mathrm{f}) = \mathbf{x}_\mathrm{f} \tag{30d}$$
$$\tilde{\mathbf{x}} \in [\tilde{\mathbf{x}}_\mathrm{min}, \tilde{\mathbf{x}}_\mathrm{max}] \tag{30e}$$
$$\mathbf{u}_\mathrm{c} \in [\mathbf{u}_\mathrm{c,min}(\mathbf{x}), \mathbf{u}_\mathrm{c,max}(\mathbf{x})] \tag{30f}$$
$$u_\sigma, u_\mathrm{g} \in \{-1, 0, 1\}, \tag{30g}$$

with $\tilde{\mathbf{x}} = (E_\mathrm{V}, \mathbf{x}_\mathrm{d})$, is solved iteratively. After the start of the algorithm, a subprogram solves the problem (30) for the whole horizon without constraints on $E_\mathrm{S}$ and for initially guessed values for $\psi_\mathrm{t}$ and $\psi_\mathrm{S}$. Subsequently, $\psi_\mathrm{t}$ is iterated using the bisection method until $t(N_\mathrm{k}) \approx t_\mathrm{f}$, where $t_\mathrm{f}$ is the final constraint on the travel time. The value for $\psi_\mathrm{S}$ is found in the same way. The initial values for the costates determine whether the algorithm will converge and how many iterations are needed to come to a solution. Thus, usable initial values are found performing a parameter variation. As a result, the values $\psi_\mathrm{t}(k_0) = 0$ and $\psi_\mathrm{S}(k_0) = -2.5$ are used here. Additionally, it is not always possible to exactly meet the final constraints because of non-linearities in the model, which is, for instance, discussed in [33]. Hence, the subprogram exits after a finite number of iterations and selects the solution closest to the final constraints.

If $E_\mathrm{S}$ computed by the subprogram is not within the state limits for all $k$, the segment's final point $k_\mathrm{f}$ is set to $\hat{k}$ which is the point at which the limits are exceeded the most (see [50]). At $\hat{k}$, the final state condition is set to the respective limit. If $E_\mathrm{S}$ of the shortened segment violates the state bounds again, the segment is split again in two parts and the procedure is repeated. Otherwise, the next decision block checks whether the current segment is the last. If this is not the case, the segment from the actual $k_\mathrm{f}$ to the final point of the horizon will be computed and if necessary split again. The process is continued until the control trajectory for the whole horizon is calculated. In order to determine the solution quality of the control trajectory yielded, the next section presents a case study.

**Remark 3.** *Problem (30) does not include any consideration for drivability and driver discomfort. However, it is conceptually straightforward to include a penalty on high acceleration with a negligible increase in computational effort. Other drivability aspects, such as penalty on longitudinal jerk, are computationally more expensive, since they require an additional state in the problem.*

## V. Case Study

Here, the implemented PMP-DP (Section IV) is assessed by comparing its results with the benchmark solution (Section III) and by estimating its computational effort at a rapid control prototyping unit.

TABLE I
State quantization for simulation.

| State | Step Size | Grid Points | |
|---|---|---|---|
| $t$ | 0.01 s | 4949 | (only DP) |
| $E_\mathrm{S}$ | 5 kJ | 271 | (only DP) |
| $E_\mathrm{V}$ | 5 kJ | 25 | |
| $g$ | 1 | 6 | |
| $\sigma$ | 1 | 2 | |

### A. Setup

The model in Section (II-A) is parameterized with the properties of a large passenger car with a mass of 1800 kg including a battery with a maximum energy of about 0.5 kWh. The power output of the ICE is 221 kW and of the EM is 28 kW.

The sample data used was recorded during a test drive with a passenger car on a randomly selected interurban route in Germany. The car's navigation system provides prediction data specified by the Advanced Driver Assistance Systems Interface Specifications (ADASIS) protocol [5], [40] to the vehicle bus. ADASIS includes information about velocity restrictions, curvature and slope for an upcoming horizon of 8.2 km at maximum. As a reason of the computational effort and resulting calculation time of the DP, only 5 km of such a horizon with one set of starting values ($v = 30$ km/h, $SoE = 50\%$, $t = 0$, $g = 2$, $\sigma = 0$) are computed for all possible final states.

The restrictions on velocity and the maximal apex speed given by the sample data are used to compute an upper kinetic energy state bound. A vehicle moving relatively slow becomes an obstacle for traffic participants. This is the reason why a positive lower bound on kinetic energy is also imposed. To obtain it, 120 kJ are subtracted from the upper bound which corresponds to a deviation of about 9 km/h when the upper velocity limit is 100 km/h. Additionally, this lower bound decreases the number of transitions that need to be computed and thereby the computational effort.

### B. Implementation

For simulation, the velocity bounds and the road slope are discretized with a step size of $\Delta s = 10$ m and the states are quantized with the values shown in Table I. Note that the travel time state with its large number of grid points has the biggest impact on the computational time of the DP. However, this fine quantization is selected to keep the discretization error of $t$ small. The quantization values of $E_\mathrm{S}$ and $E_\mathrm{V}$ are chosen to compute the benchmark solution in a reasonable amount of time. Although a finer quantization would yield even better results the chosen quantization is sufficient for comparison, since both approaches use the same values.

In this paper, the benchmark solution as well as the PMP-DP are coded in MATLAB[1] and implemented in forward direction.

### C. Solution Quality

In order to compare the solution quality, results for a set of different final conditions (travel time and SoE) are computed

[1] MATLAB is a registered trademark of The MathWorks, Inc.

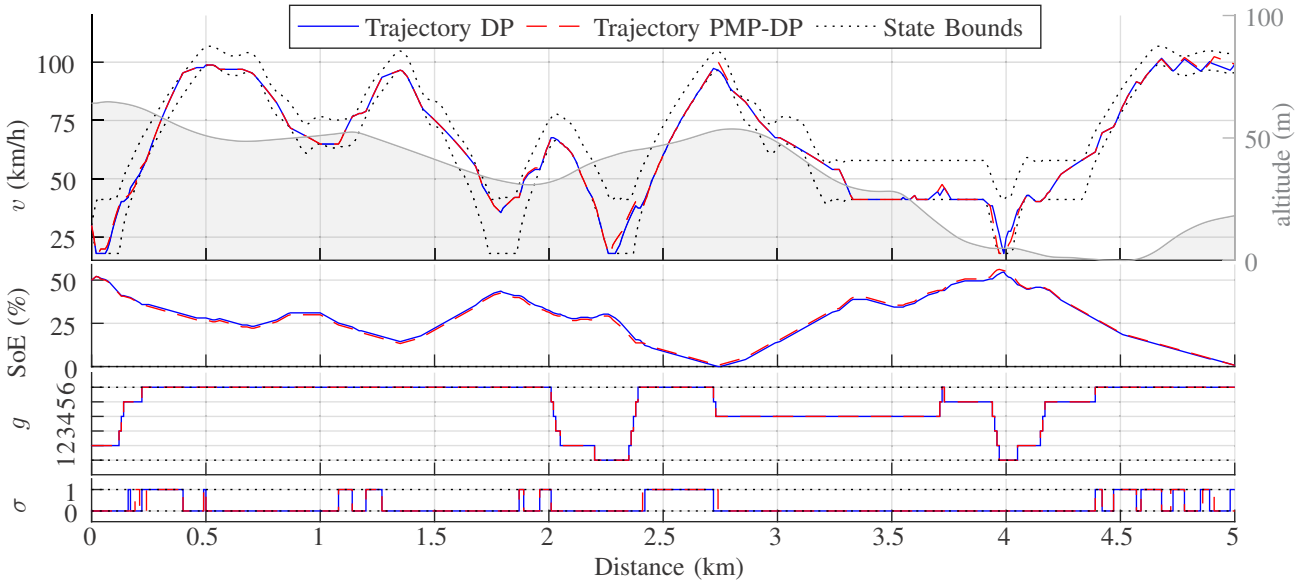


Fig. 6. Comparison of both methods for full discharge of the battery. The continuous states in the two upper plots show only slight differences in behavior as well as the engine state decision (see fourth plot from the top), while the gear trajectories (third plot) are equal.

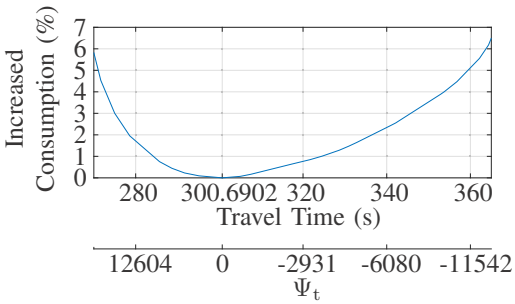


Fig. 7. Fuel consumption over travel time for balanced SoE (50 %). Due to bounds for the minimal kinetic energy (see. Fig. 6) which enforce a worse velocity trajectory, the best point is not the longest travel time (slowest average speed). This is why the costate of the time shown in the second axis has to be negative to reward going slower. Consequently, the value $\psi_t = 0$ yields the lowest fuel consumption.

TABLE II
DECLINE IN SOLUTION QUALITY OF THE PMP-DP (%).

| Final SoE | Travel Time | | | | | |
|---|---|---|---|---|---|---|
| (%) | 270 s | 280 s | 300 s | 320 s | 340 s | 360 s |
| 0 | 1.63 | 2.18 | 2.19 | 2.18 | 2.47 | 2.15 |
| 25 | -0.04 | -0.02 | 0 | -0.02 | -0.01 | 0 |
| 50 | -0.06 | -0.01 | 0 | 0 | 0.03 | 0 |
| 75 | -0.17 | 0.04 | 0.06 | 0.15 | 0.13 | 0.02 |
| 100 | 1.21 | 0.3 | 0.48 | 0.26 | 0.17 | 1.26 |

with DP and PMP-DP. For each comparison both methods use the same initial and final states. To give an understanding of the different scenarios, one with a relative poor result is depicted in Fig. 6. Here, the kinetic energy state is represented by the velocity shown in the top plot together with the state bounds and the road altitude.

The second plot from the top in Fig. 6 illustrates the battery energy and its limits which are reached at 2.7 km causing a segmentation of the PMP-DP (explained in Fig. 5). It is pointed out, that the integer states in plots 3 and 4 from the top in Fig. 6 make only a few changes due to the penalty factors $\beta_g$ and $\beta_\sigma$. Omitting these terms would lead to frequent changes of $g$ and $\sigma$ because they would adopt their respective best value at every instant.

Note, that $\psi_t = 0$ leads to the lowest fuel consumption but does not yield the longest travel time. This behavior which is shown in Fig. 7 is caused by the minimum state bound for $E_V$ that enforces at some sections operating points where the drive units have a poorer efficiency.

In the example shown in Fig. 6 the ICE is only turned on a few times because most of the propulsion energy comes from the battery. This leads to a low fuel consumption so that the slight differences of the state trajectories, shown in the upper four plots, yield a relative big error of 2.36 % in solution quality. This is confirmed when looking at Table II which shows the decline in fuel consumption by the PMP-DP for different values of travel time and final SoE. Note, that PMP-DP cannot ensure meeting the final conditions exactly. Thus, the corresponding benchmark solution yielding the same values is picked for comparison. It can be seen that PMP-DP, which does not suffer from a discretization error of the time state, yields even better results than the benchmark solution (negative decline). The highest difference occurs for minimum and maximum final SoE, since in these scenarios the battery energy bounds are hit. However, even in these scenarios the error is negligible, as it can be observed in Fig. 6 that the state and control trajectories between the proposed and the benchmark solutions almost completely overlap.

### D. Computational Effort

Solving the proposed PMP-DP method required about 60 s on a personal computer[2]. The benchmark method is computa-

[2] A Lenovo Thinkpad T430s with an Intel Core i5-3320M and 16 GB RAM is used.

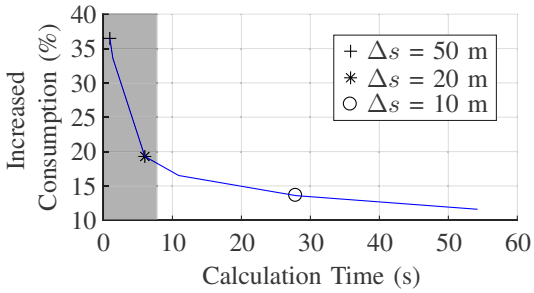


Fig. 8. Additional fuel consumed compared to the solution with the finest discretization over calculation time of one iteration for different $\Delta s$ for balanced SoE (50 %). Values are calculated on the RPCU. The calculation time which is assumed to be online capable is shown by the shaded area.

tionally more challenging and it has therefore been solved on a high performance computer (HPC) cluster[3]. Yet, obtaining the globally optimal solution with DP required about 124 days.

It has been observed that PMP-DP needed less than 15 iterations for obtaining a solution within 3 s tolerance in travel time and 1 % in final SoE. Yet, the computational effort with the current settings is too high to allow an online usage of PMP-DP. Decreasing the computational load is possible, by e.g. increasing the sampling interval, decreasing the prediction horizon, or decreasing the resolution of state quantization.

Fig. 8 shows the solution quality for different step sizes of $\Delta s$ computed at a rapid prototyping control unit[4] (RPCU). Due to an excessive computational effort, results for the reference with finest discretization ($\Delta s = 1m$) are computed using the HPC. For the same reason the HPC was used in advance to perform a comprehensive variation of $\Delta s$, $\Delta E_{\mathrm{S}}$ and $\Delta E_{\mathrm{V}}$. As a result, the same values for $\Delta E_{\mathrm{S}}$ and $\Delta E_{\mathrm{V}}$ shown in Table I are used for the assessment with the RPCU as well. To determine online capability it is estimated how long the calculation of one iteration is allowed to take. When driving with a velocity of 150 km/h the vehicle needs 120 s for a 5 km horizon. Assuming the maximum of 15 iterations, to come to a solution, each one should be calculated in less than 8 s at the RPCU. As shown in Fig. 8 the PMP-DP can possibly be used online when accepting about 17 % higher fuel consumption compared to the one with the finest discretization, which is calculated with the HPC.

## VI. Conclusion and Future Research

This paper presented a novel method that solves the five state mixed-integer problem over one hundred thousand times faster than the benchmark method with nearly the same solution quality. The computational effort of the PMP-DP can be adjusted by varying the sampling of the position so that it can even be used on a vehicle control unit.

Future research will focus on further decreasing the computational effort and improving the driveability. A huge benefit in calculation time can be expected when succeeding to solve the problem only with PMP (27), since the DP causes most of the computational effort. On that account, it is necessary to find an approximation for the dynamic equation of the kinetic energy costate. In this context, the integer decisions have to be considered as control signals, rather than states, whose effect on the solution quality and computational time has to be studied as well.

[3]One node with 24 cores (Intel E5-2690) and 5 GB RAM per Core were used on the Bull HPC-Cluster (Taurus) at The Center for Information Services and High Performance Computing (ZIH) at Technische Universität Dresden

[4]DSpace MicroAutoboxII

## References


[1] R. Bellman, "The theory of dynamic programming," *Bull. Amer. Math. Soc.*, pp. 503–515, 1954, ISSN: 0002-9904.

[2] D. P. Bertsekas, *Dynamic programming and optimal control*, 3rd ed, ser. Athena Scientific optimization and computation series. Athena Scientific, 2005-2007, ISBN: 1-886529-26-4.

[3] T. J. Böhme and B. Frank, *Hybrid systems, optimal control and hybrid vehicles: Theory, methods and applications*, ser. Advances in industrial control. 2017, ISBN: 978-3-319-51317-1.

[4] S. Boyd and L. Vandenberghe, *Convex Optimization*. Cambridge University Press, 2004, ISBN: 0521833787.

[5] A. Bracht, *Adasis v2 protocol: version 2.03.0*, 2013.

[6] L. Bühler, *Fuel-efficient platooning of heavy duty vehicles through road topography preview information*, 2013.

[7] S. Delprat, J. Lauber, T. M. Guerra, and J. Rimaux, "Control of a parallel hybrid powertrain: optimal control," vol. 53, no. 3, pp. 872–881, 2004.

[8] W. Dib, L. Serrao, and A. Sciarretta, Eds., *Optimal control to minimize trip time and energy consumption in electric vehicles*, 2011.

[9] P. Elbert, T. Nüesch, A. Ritter, N. Murgovski, and L. Guzzella, "Engine on/off control for the energy management of a serial hybrid electric bus via convex optimization," vol. 63, no. 8, pp. 3549–3559, 2014.

[10] F. Flehmig, F. Kästner, K. Knödler, and M. Knoop, "Eco-acc für elektro- und hybridfahrzeuge," vol. 116, no. 4, pp. 22–27, 2014.

[11] O. Föllinger, *Optimale Regelung und Steuerung*. R. Oldenbourg Verlag, 1994.

[12] S. Gonsrang, "Optimization-based energy management system for pure electric vehicles," in *Energy Efficient Vehicles 2015*, vol. 5, pp. 100–110.

[13] L. Guzzella and A. Sciarretta, *Vehicle propulsion systems: Introduction to modeling and optimization*, 2nd ed. Springer, 2007, ISBN: 978-3-540-74691-1.

[14] Hans Peter Geering, *Optimal Control with Engineering Applications*. Springer-Verlag, 2007.

[15] M. Helbing, *Energiemanagement für eine parallele hybridarchitektur*, 2014.

[16] E. Hellström, J. Aslund, and L. Nielsen, "Design of an efficient algorithm for fuel-optimal look-ahead control," vol. 18, no. 11, pp. 1318–1327, 2010.

[17] E. Hellström, M. Ivarsson, J. Aslund, and L. Nielsen, "Look-ahead control for heavy trucks to minimize trip time and fuel consumption," vol. 17, no. 2, pp. 245–254, 2009.

[18] P. Hofmann, *Hybridfahrzeuge: Ein alternatives Antriebssystem für die Zukunft*, 2. Auflage. 2014, ISBN: 978-3-7091-1779-8.

[19] B. d. Jager, T. van Keulen, and J. Kessels, *Optimal control of hybrid vehicles*, ser. Advances in industrial control. Springer, 2013, ISBN: 978-1-4471-5075-6.

[20] L. Johannesson, N. Murgovski, E. Jonasson, J. Hellgren, and B. Egardt, "Predictive energy management of hybrid long-haul trucks," vol. 41, pp. 83–97, 2015.

[21] L. Johannesson, M. Nilsson, and N. Murgovski, Eds., *Look-ahead vehicle energy management with traffic predictions*, vol. 48, 2015.

[22] . A. S. Kamal, M. Mukai, J. Murata, and T. Kawabe, "Model predictive control of vehicles on urban roads for improved fuel economy," vol. 21, no. 3, pp. 831–841, 2013.

[23] S. Kutter and B. Bäker, Eds., *An iterative algorithm for the global optimal predictive control of hybrid electric vehicles*, 2011.

[24] S. Kutter, "Eine prädiktive und optimierungsbasierte betriebsstrategie für autarke und extern nachladbare hybridfahrzeuge," Technische Universität Dresden, Dresden, 2013.

[25] K.-Y. Liang, J. Mårtensson, and K. H. Johansson, "Power management strategy for a parallel hybrid electric truck," 2003.

[26] A. A. Malikopoulos, "Supervisory power management control algorithms for hybrid electric vehicles: a survey," *IEEE Transactions on Intelligent Transportation Systems*, vol. 15, no. 5, pp. 1869–1885, 2014, ISSN: 1524-9050.

[27] S. Mulder, *Energy management strategy for a hybrid container crane*, 2009.

[28] N. Murgovski, L. M. Johannesson, and J. Sjoberg, "Engine on/off control for dimensioning hybrid electric powertrains via convex optimization," vol. 62, no. 7, pp. 2949–2962, 2013.

[29] N. Murgovski, B. Egardt, and M. Nilsson, "Cooperative energy management of automated vehicles," *Control Engineering Practice*, vol. 57, pp. 84–89, 2016, ISSN: 0967-0661.

[30] N. Murgovski, L. Johannesson, J. Sjöberg, and B. Egardt, "Component sizing of a plug-in hybrid electric powertrain via convex optimization," vol. 22, no. 1, pp. 106–120, 2012.

[31] N. Murgovski, J. Sjöberg, and J. Fredriksson, "A methodology and a tool for evaluating hybrid electric powertrain configurations," vol. 3, no. 3, pp. 219–245, 2011.

[32] C. Musardo, G. Rizzoni, Y. Guezennec, and B. Staccia, "A-ecms: an adaptive algorithm for hybrid electric vehicle energy management," vol. 11, no. 4–5, pp. 509–524, 2005.

[33] Ngo Dac Viet, *Gear shift strategies for automotive transmissions*, 2012.

[34] T. Nüesch, P. Elbert, M. Flankl, C. Onder, and L. Guzzella, "Convex optimization for the energy management of hybrid electric vehicles considering engine start and gearshift costs," vol. 7, no. 2, p. 834, 2014.

[35] G. Paganelli, T. M. Guerra, S. Delprat, J.-J. Santin, M. Delhom, and E. Combes, "Simulation and assessment of power control strategies for a parallel hybrid car," vol. 214, no. 7, pp. 705–717, 2000.

[36] L. S. Pontryagin, V. G. Boltyanskii, R. V. Gamkrelidze, and E. F. Mishchenko, *The Mathematical Theory of Optimal Processes*. Interscience Publishers, 1962.

[37] M. Pourabdollah, N. Murgovski, B. S. Egardt, and A. Grauers, "An iterative dynamic programming/convex optimization procedure for optimal sizing and energy management of phevs," in *The 19th World Congress of the International Federation of Automatic Control*, pp. 6606–6611.

[38] M. Pourabdollah, N. Murgovski, A. Grauers, and B. Egardt, "Optimal sizing of a parallel phev powertrain," vol. 62, no. 6, pp. 2469–2480, 2013.

[39] T. Radke, *Energieoptimale Längsführung von Kraftfahrzeugen durch Einsatz vorausschauender Fahrstrategien*. KIT Scientific Publishing, 2013, ISBN: 978-3-7315-0069-8.

[40] C. Ress, D. Balzer, A. Bracht, S. Durekovic, and J. Löwenau, *Adasis protocol for advanced in-vehicle applications*, 2008.

[41] A. A. Robichek, E. J. Elton, and M. J. Gruber, "Dynamic programming applications in finance," vol. 26, no. 2, pp. 473–506, 1971.

[42] Rui Wang and S. M. Lukic, Eds., *Dynamic programming technique in hybrid electric vehicle optimization*, 2012.

[43] A. B. Schwarzkopf and R. B. Leipnik, "Control of highway vehicles for minimum fuel consumption over varying terrain," vol. 11, no. 4, pp. 279–286, 1977.

[44] A. Sciarretta, G. D. Nunzio, and L. L. Ojeda, "Optimal ecodriving control: energy-efficient driving of road vehicles as an optimal control problem," vol. 35, no. 5, pp. 71–90, 2015.

[45] O. Sundstrom and L. Guzzella, Eds., *A generic dynamic programming Matlab function*, 2009.

[46] E. D. Tate and S. P. Boyd, Eds., *Finding Ultimate Limits of Performance for Hybrid Electric Vehicles*, 2000.

[47] C. Tempelhahn, S. Uebel, and B. Bäker, "State of the art in optimal control of series hybrid electric vehicles taking account of driveability," in *Proceedings EEHE Wiesloch 2016*.

[48] P. Themann, A. Zlocki, and L. Eckstein, "Energieeffiziente fahrzeuglängsführung durch v2x-kommunikation," vol. 116, no. 7-8, pp. 62–67, 2014.

[49] S. Uebel, C. Tempelhahn, M. Liebers, S. Kutter, and B. Bäker, "Anwendung der variationsrechnung für steuerungsaufgaben im kraftfahrzeug," *at - Automatisierungstechnik*, vol. 62, 2014.

[50] T. van Keulen, J. Gillot, B. d. Jager, and M. Steinbuch, "Solution for state constrained optimal control problems applied to power split control for hybrid vehicles," vol. 50, no. 1, pp. 187–192, 2014.

[51] T. van Keulen, B. d. Jager, D. Foster, and M. Steinbuch, Eds., *Velocity trajectory optimization in hybrid electric trucks*, 2010.

[52] T. van Keulen, B. d. Jager, and M. Steinbuch, Eds., *Optimal Trajectories for Vehicles with Energy Recovery Options*, 2011.

[53] H.-G. Wahl, K.-L. Bauer, F. Gauterin, and M. Holzapfel, Eds., *A real-time capable enhanced dynamic programming approach for predictive optimal cruise control in hybrid electric vehicles*, 2013.

[54] K. Yu, Q. Liang, J. Yang, and Y. Guo, "Model predictive control for hybrid electric vehicle platooning using route information," pp. 1–13, 2015.

**Stephan Uebel** received his diploma in mechatronics from the Technische Universität Dresden in 2010. There, he is currently working towards his PhD degree in the field of optimal control of hybrid electric vehicles at the Chair of Vehicle Mechatronics.

**Nikolce Murgovski** received the M.Sc. degree in Software Engineering from University West, Sweden, 2007, the M.Sc. degree in Applied Physics in 2007 and the Ph.D. degree in Signals and Systems in 2012, both at Chalmers University of Technology, Sweden. Currently he is an Assistant Professor at the Department of Signals and Systems at Chalmers University. His main areas of interest include optimization and optimal control in the automotive area.

**Conny Tempelhahn** recieved the diploma in mechatronics from Technische Universität Dresden in 2011. There, he is currently working towards his PhD degree in the field of optimal control of hybrid electric vehicles at the Chair of Vehicle Mechatronics.

**Bernard Bäker** is professor and head of the Chair of Vehicle Mechatronics at Institute of Automobile Engineering at the Technische Universität Dresden. Core competencies and research fields are inter alia: Alternative Drive Trains; Assistance Systems; Diagnosis and Test of Mechatronic Systems; E/E-Architecture Development, Energetic Management; as well as Energy Systems.